Non-Abelian Holonomy of Majorana Zero Modes Coupled to a Chaotic Quantum Dot

Max Geier,[1] Svend Krøjer,[1] Felix von Oppen,[2] Charles M. Marcus,[1] Karsten Flensberg,[1] and Piet W. Brouwer[2]
[1]Center for Quantum Devices, Niels Bohr Institute, University of Copenhagen, DK-2100 Copenhagen, Denmark
[2]Dahlem Center for Complex Quantum Systems and Physics Department, Freie Universität Berlin, Arnimallee 14, 14195 Berlin, Germany

(Received 20 April 2023; revised 24 October 2023; accepted 16 December 2023; published 19 January 2024)

If a quantum dot is coupled to a topological superconductor via tunneling contacts, each contact hosts a Majorana zero mode in the limit of zero transmission. Close to a resonance and at a finite contact transparency, the resonant level in the quantum dot couples the Majorana modes, but a ground-state degeneracy per fermion parity subspace remains if the number of Majorana modes coupled to the dot is five or larger. Upon varying shape-defining gate voltages while remaining close to resonance, a nontrivial evolution within the degenerate ground-state manifold is achieved. We characterize the corresponding non-Abelian holonomy for a quantum dot with chaotic classical dynamics using random matrix theory and discuss measurable signatures of the non-Abelian time evolution.

DOI: 10.1103/PhysRevLett.132.036604

Billiards are among the simplest physical systems that exhibit chaotic dynamics if the boundary is of sufficiently irregular shape [1]. When the motion of the particle in the billiard is coherent, the statistics of its energy eigenvalues follows a universal law [2] that, depending on the particle's spin and the presence of time-reversal symmetry, derives from one of the three Wigner-Dyson random matrix ensembles [3,4]. An "electron billiard"—a quantum dot (QD)—coupled to a superconductor confines quasiparticles by Andreev reflection [5]. The chaotic quantum dynamics of such "Andreev billiards" [6–9] are described by novel random matrix ensembles, exhaustively contained in the tenfold-way classification [10].

Here, we consider a chaotic QD coupled to a *topological* superconductor, so that reflection at the boundary allows tunneling into Majorana zero modes (MZMs). We show that for weak coupling and close to a resonance, such a system has a degenerate ground-state manifold with non-Abelian evolution under generic cyclic adiabatic changes of the dot shape if the number of coupled separated MZMs, N, is five or larger. The holonomy of closed loops in "shape space" inherits its statistical distribution from the universal statistics of QD wave functions.

Demonstrating non-Abelian properties of MZMs remains an open milestone. Other approaches, such as braiding or fusion [11], require strong direct manipulations of the MZMs. This may be challenging due to the sensitivity of MZMs to disorder [12,13]. Our approach eases these requirements by coupling only perturbatively to the MZMs and driving nonlocally via the QD.

A schematic picture of the QD is shown in Fig. 1. The MZMs $\hat{\gamma}_j$, $j = 1, \ldots, N$ are located at tunneling contacts to a topological superconductor. For weak coupling, if the Fermi energy is close to a QD resonance, hybridization between MZMs and QD is dominated by a single dot level and may be described by the Hamiltonian [14,15]

$$\hat{H} = \varepsilon \hat{c}^\dagger \hat{c} + \sum_{j=1}^{N} (v_j^* \hat{c}^\dagger - v_j \hat{c}) \hat{\gamma}_j, \tag{1}$$

where $\hat{c}^\dagger$ and $\hat{c}$ are creation and annihilation operators of the resonant level, ε is its energy (relative to the Fermi level), and the v_j are complex coefficients describing tunneling between the dot level and the MZMs. Neglecting hybridization with nonresonant levels, only two linearly independent superpositions of MZMs hybridize with the dot mode and acquire a finite energy. The remaining $N - 2$ MZMs are "dark" modes, which remain at zero energy despite being coupled to the dot. The Hamiltonian (1) is easily diagonalized and one obtains the dark modes $\hat{\Gamma}_i$ as superpositions of the original MZMs

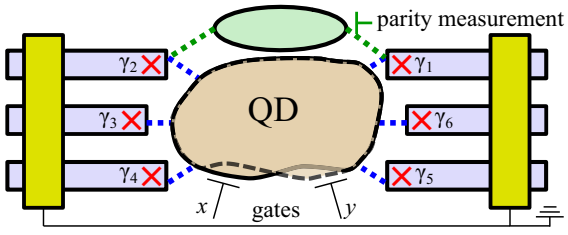

FIG. 1. N MZMs $\hat{\gamma}_j$ supported by a grounded topological superconductor are tunnel-coupled to a chaotic QD. The dot shape can be changed by two gates with dimensionless voltages x and y, whereas a third gate allows for a uniform shift of the dot potential. A parity measurement involving two of the MZMs allows for the detection of non-Abelian evolution resulting from a closed loop in "shape space".

$\hat{\Gamma}_i = \sum_{j=1}^{N} o_{ji}\hat{\gamma}_j$, $i = 1, \ldots, N-2$, with real coefficients o_{ij} satisfying the (complex) orthogonality condition

$$\sum_{j=1}^{N} o_{ji} v_j = 0. \tag{2}$$

Changing the shape of the dot, while keeping ε close to zero, changes its eigenmodes and, hence, the tunneling amplitudes v_j between the resonant mode and the MZMs. (Keeping ε close to zero requires adjusting a third gate voltage while performing the shape change.) Via the orthogonality condition (2), adiabatically changing the dot shape therefore leads to an adiabatic change of the subspace spanned by the $N-2$ dark MZMs. A loop $\mathcal{C}$ in "billiard shape space," which returns the dot to its original shape, may nevertheless lead to a "rotation" in the space of the $N-2$ dark MZMs,

$$\Gamma_j \to \sum_{k=1}^{N-2} W_{kj}\Gamma_k, \tag{3}$$

where the matrix $W \in \mathrm{SO}(N-2)$ is known as the "holonomy" of the loop $\mathcal{C}$. For $N \geq 5$, the group $\mathrm{SO}(N-2)$ is non-Abelian, so that holonomies of different loops in shape space generally do not commute [16].

Wave functions of a chaotic QD and their response to a change of the dot shape are random, with a universal statistical distribution described by random matrix theory [17–19]. As a result, the holonomy W of a loop in "shape space" is also a random quantity with universal statistics. We consider a QD with two parameters x and y that determine its shape. In random matrix theory, the "shape coordinates" x and y are dimensionless, normalized such that a change $\Delta x, y \sim 1$ corresponds to an effective "scrambling" of the spectrum [18–21]. In the remainder of this Letter, we determine the universal distribution of the holonomy W for small and large loops in "shape space." We propose two observables of the non-Abelian holonomy for $N \geq 5$—a "fermion parity signature" and a "charge signature"—and show that these have universal statistics for a chaotic QD.

Holonomy.—We consider a QD with two parameters x and y determining its shape. Hence, "shape space" is the two-dimensional plane, parametrized by "shape coordinates" x and y. A loop therein is parametrized by $x(\tau), y(\tau)$, $0 \leq \tau \leq 1$, with $x(0) = x(1) = 0$, $y(0) = y(1) = 0$. The corresponding holonomy matrix $W \in \mathrm{SO}(N-2)$ results from the Wilson loop operator [22] $\mathcal{W} = \mathcal{L}_\tau e^{-\int_0^1 d\tau \mathcal{P}(x,y) d\mathcal{P}(x,y)/d\tau \mathcal{P}}$, where $\mathcal{P}(x,y)$ is the projector on the $(N-2)$-dimensional subspace of dark MZMs, we abbreviated $\mathcal{P} = \mathcal{P}(0,0)$, and $\mathcal{L}_\tau$ denotes path ordering, such that factors with lower τ appear to the right of factors with higher τ. To remain within the dark space, the loop in parameter space must be performed slowly on the timescale associated with coupling to the resonant level, but fast compared to the timescale related to the coupling to the nonresonant levels. For an infinitesimal shape-space loop with enclosed area A, the Wilson loop operator takes the form

$$\mathcal{W} \simeq e^{wA}\mathcal{P}, \qquad w = \mathcal{P}[\partial\mathcal{P}/\partial y, \partial\mathcal{P}/\partial x]\mathcal{P}, \tag{4}$$

where $w = \mathcal{P}(\partial_x \mathcal{A}_y - \partial_y \mathcal{A}_x + i[\mathcal{A}_x, \mathcal{A}_y])\mathcal{P}$ is the projected non-Abelian field strength associated to the gauge field $\mathcal{A}_\rho = \mathcal{P}\partial_\rho\mathcal{P}$, $\rho = x, y$. The dark subspace is defined by the orthogonality condition (2). The projection operator $\mathcal{P}$ can be expressed in terms of the N-component vector $\mathbf{v} = (v_1, \ldots, v_N)$, $\mathcal{P} = \mathbb{1}_N - (2\mathcal{Q}/\mathrm{tr}\mathcal{Q})$, where $\mathbb{1}_N$ is the $N \times N$ unit matrix and $\mathcal{Q} = \mathrm{Re}[\mathbf{v}(\mathbf{v}^\dagger\mathbf{v})\mathbf{v}^\dagger - \mathbf{v}(\mathbf{v}^\dagger\mathbf{v}^*)\mathbf{v}^\mathrm{T}]$. For the generator w of the holonomy one then obtains (for details, see Supplemental Material [23])

$$w = \frac{2\mathcal{P}}{\mathrm{tr}\mathcal{Q}}\mathrm{Re}[\mathbf{d}_x^*(\mathbf{v}^\dagger\mathbf{v})\mathbf{d}_y^\mathrm{T} - \mathbf{d}_x(\mathbf{v}^\dagger\mathbf{v}^*)\mathbf{d}_y^\mathrm{T} - (x \leftrightarrow y)]\mathcal{P}, \tag{5}$$

where we abbreviated $\mathbf{d}_x = \partial\mathbf{v}/\partial x$, $\mathbf{d}_y = \partial\mathbf{v}/\partial y$. The matrix elements W_{kj} of Eq. (3) are found by the projection of $\mathcal{W}$ onto the dark MZM wave functions, $W_{kj} = \sum_{n,m=1}^{N} o_{mk}\mathcal{W}_{mn}o_{nj}$.

Statistics of the holonomy.—The statistics of the coefficients v_j and their dependence on the two shape parameters x and y can be obtained by modeling the Hamiltonian of the dot, without coupling to the superconductors, as an $M \times M$ random hermitian matrix [17,18],

$$H(x,y) = H_0 + \frac{1}{\sqrt{M}}(xH_x + yH_y). \tag{6}$$

Assuming broken time reversal and lifted spin degeneracy, e.g., by the Zeeman coupling to an applied magnetic field [31], the matrices H_0, H_x, and H_y are statistically independent and taken from the Gaussian unitary ensemble. The normalization factors $\sqrt{M}$ are included such that the results become independent of M as $M \to \infty$. The resonant dot mode is identified with the mth eigenstate of H, with eigenvalue $\varepsilon \equiv \varepsilon_m$ and $m \sim M/2$ near the center of its spectrum. Its eigenket $|\varepsilon_m\rangle$ determines the complex coefficients $v_j = \eta_j\langle j|\varepsilon_m\rangle\sqrt{M}$, where η_j is a proportionality factor depending on the QD level spacing δ, superconducting gap Δ_j and normal-state transmission coefficient $T_j \ll 1$ of the jth tunnel contact to a MZM with wave function $|j\rangle$. The coefficients v_j have independent Gaussian distributions with zero mean and with variance $\langle|v_j|^2\rangle = \eta_j^2$. The derivatives $\mathbf{d}_{x,y}$ follow from first-order perturbation theory in H_x and H_y,

$$\mathbf{d}_{x,y} = \frac{1}{\sqrt{M}}\sum_{k\neq m}\frac{\langle\varepsilon_k|H_{x,y}|\varepsilon_m\rangle}{\varepsilon_k - \varepsilon}\mathbf{v}_k, \tag{7}$$

where ε_k, $k \neq m$, are the other eigenvalues of H and $|\varepsilon_k\rangle$ and $\mathbf{v}_k$ the corresponding eigenket and vector of coupling coefficients, respectively. The matrix elements $\langle\varepsilon_k|H_{x,y}|\varepsilon_m\rangle$ are independently distributed complex Gaussian random numbers with zero mean and with variance $M\delta^2/\pi^2$. The vectors $\mathbf{v}_k$ are statistically independent and have the same distribution as $\mathbf{v} \equiv \mathbf{v}_m$.

To find the statistical distribution of the generator w of the holonomy, we make the additional assumption that all N tunnel contacts have the same proportionality constants $\eta \equiv \eta_j$. Then, from a statistical point of view, the MZMs are interchangeable. With this simplifying assumption, the complex coefficients v_j have Gaussian distributions with the same variance and the distributions of the N-component vector $\mathbf{v}$ and its derivatives $\mathbf{d}_{x,y}$ are separately invariant with respect to unitary transformations. It then follows that w is an $(N-2)\times(N-2)$ antisymmetric real matrix of the form

$$w = \begin{cases} 0 & \text{if } N = 3, \\ i\lambda\sigma_y & \text{if } N = 4, \\ i\lambda O\,\mathrm{diag}(\sigma_y, 0)O^{\mathrm{T}} & \text{if } N = 5, \\ iO\,\mathrm{diag}(\lambda_1\sigma_y, \lambda_2\sigma_y)O^{\mathrm{T}} & \text{if } N = 6, \\ iO\,\mathrm{diag}(\lambda_1\sigma_y, \lambda_2\sigma_y, 0, \ldots)O^{\mathrm{T}} & \text{if } N > 6, \end{cases} \tag{8}$$

where σ_y is the Pauli matrix and $O \in \mathrm{SO}(N-2)$ is uniformly distributed. In contrast, the principal values λ_j of the holonomy generator w have nontrivial and distinctive statistical distributions. Figure 2 displays the numerically sampled probability distribution functions (PDFs) $P(\lambda)$ (for $N = 4, 5$) and $P(\lambda_1, \lambda_2)$ (for $N = 6, 10$). For $N = 5$, $P(\lambda) \propto \lambda^2$ for small λ. For $N \geq 6$, $P(\lambda_1, \lambda_2)$ exhibits quadratic level repulsion $\propto |\lambda_2 - \lambda_1|^2$ for $\lambda_1 \approx \lambda_2$, in agreement with the result for real skew-symmetric matrices [10], and a power-law repulsion from the coordinate axes following $P(\lambda_1, \lambda_2) \propto \lambda_1^{N-6}\lambda_2^{N-6}$ for $|\lambda_1| \ll 1$ or $|\lambda_2| \ll 1$. For large values, the PDFs of λ (for $N = 4, 5$) and of $\lambda \equiv \max(\lambda_1, \lambda_2)$ have an algebraic tail $\propto \lambda^{-5/2}$ [32], which can be traced back to rare events with a small spacing between $\varepsilon = \varepsilon_m$ and the neighboring dot levels ε_{m-1} or ε_{m+1} [33–36].

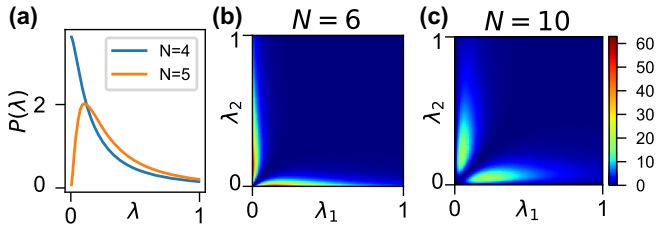

FIG. 2. PDFs $P(\lambda)$ (for $N = 4, 5$ MZMs coupled to the dot) and $P(\lambda_1, \lambda_2)$ (for $N = 6, 10$) of the principal values of the holonomy generator w. The statistical ensemble used to sample the distributions consists of 10^7 realizations of the random matrix model (6) with matrix size $M = 20$.

For loops with small area in shape space, the distribution of the holonomy matrix W is found by exponentiating the generator w, see Eq. (4), and its statistical distribution follows accordingly. To obtain a holonomy matrix that significantly differs from the identity, one may repeat a small-area loop $Z \gg 1$ times. In this case, $W = e^{ZAw}$ is of the form $O\mathrm{diag}(e^{i\alpha_1\sigma_y}, e^{i\alpha_2\sigma_y}, 1, \ldots)O^{\mathrm{T}}$ if $N \geq 4$, where O is uniformly distributed in $\mathrm{SO}(N-2)$ and the phase angles $\alpha_j = ZA\lambda_j \bmod 2\pi$, $j = 1, 2$, are uniformly and independently distributed in the interval $(-\pi, \pi]$ if $ZA \gg 1$. (The phase angle $\alpha_2 = 0$ for $N = 4, 5$.) A large holonomy may also be obtained simply by taking a shape-space loop with large area $A \gg 1$. In this case, the holonomy matrix W itself becomes uniformly distributed in $\mathrm{SO}(N-2)$ in the limit of large A.

The holonomy W cannot be observed directly, because the dark MZMs involved in it are nonlocal modes without weight in the QD. Below we propose two measurement protocols that circumvent this problem. In the first protocol, which we refer to as "fermion parity signature," two dark MZMs are fully isolated from the chaotic dot and coupled to a small QD instead, which allows their parity to be measured. In the second protocol, referred to as "charge signature," a sudden change of the coupling parameters transfers weight from the dark MZMs to the chaotic QD, which leads to a change of the charge on the dot, which is then measured capacitively.

Fermion parity signature.—A pair of MZMs may be combined into a single (complex) fermion [37,38]. Figure 1 displays a setup that permits to observe a signature of the non-Abelian evolution through the measurement of the fermion occupation $\hat{f}_1^\dagger\hat{f}_1 = \frac{1}{2}(1 + i\hat{\gamma}_1\hat{\gamma}_2)$ of two MZMs $\hat{\gamma}_1$ and $\hat{\gamma}_2$ by coupling both MZMs to a QD [39–41]. For initialization, we take $\hat{\gamma}_1$ and $\hat{\gamma}_2$ decoupled from the chaotic dot and set the occupation $\hat{f}_1^\dagger\hat{f}_1$ to zero by a projective measurement. The "dark" MZM operators $\hat{\Gamma}_i$, $i = 1, \ldots, N-2$, then consist of $\hat{\Gamma}_1 = \hat{\gamma}_1$, $\hat{\Gamma}_2 = \hat{\gamma}_2$, as well as the operators $\hat{\Gamma}_3, \ldots, \hat{\Gamma}_{N-2}$, which are linear combinations of the MZMs $\hat{\gamma}_3, \ldots, \hat{\gamma}_N$. Their state can be initialized by letting the system relax to its unique ground state on timescales large enough that the coupling to nonresonant dot levels becomes relevant. To bring about the non-Abelian evolution, we then (i) adiabatically increase the coupling strength of $\hat{\gamma}_{1,2}$ to the dot from 0 to η, (ii) perform a loop in shape space, and (iii) again measure $\hat{f}_1^\dagger\hat{f}_1$ after decoupling $\hat{\gamma}_{1,2}$ from the dot.

Choosing the basis of the remaining dark-space MZMs such that the initial state corresponds to the vacuum for the associated fermions $\hat{f}_i = (1/2)(\hat{\Gamma}_{2i-1} + i\hat{\Gamma}_{2i})$, $i = 2, \ldots, N/2$, the probability Δp that the occupation $\hat{f}_1^\dagger\hat{f}_1$ has changed is [23]

$$\Delta p = \frac{1}{2} - \frac{1}{2}\sum_{j=1}^{N/2-1}(W_{2j,2}W_{2j-1,1} - W_{2j-1,2}W_{2j,1}). \tag{9}$$

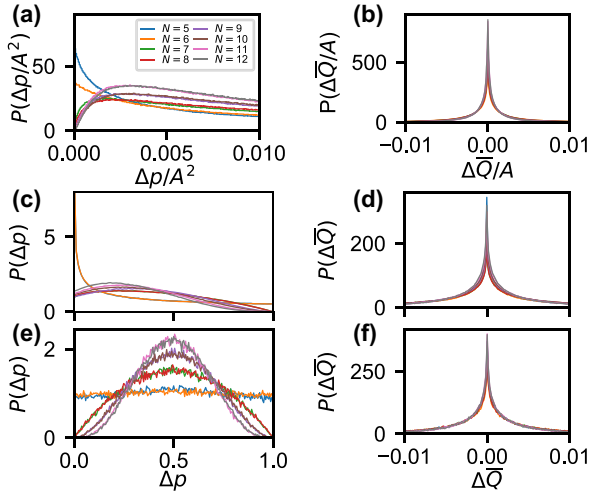

FIG. 3. Left: PDF of the parity signature Δp. Right: PDF of the charge signature $\Delta\overline{Q}$ for resonant energy $\epsilon/\eta = 2\sqrt{20} \approx 9$, obtained by suddenly decoupling two MZMs from the dot. In (a),(b), the distributions of the normalized signatures $\Delta p/A$ and $\Delta\bar{Q}/A^2$ are shown for $N = 5, 6, \ldots, 12$ and in the limit of small loop area $A \ll 1$. In (c),(d), distributions of Δp and $\Delta\bar{Q}$ are shown for repeated infinitesimal loops with $ZA = 1000$. For (a), (b) and (c),(d), distributions are obtained from 10^7 and 10^6 realizations, respectively, of the random-matrix model (6) with matrix size $M = 20$. The last row, (e),(f), shows distributions of Δp and $\Delta\bar{Q}$ for large loop area $A \gg 1$, $M = 64$, sampled over 10^5 realizations, and with $\epsilon/\eta = 16$. (See Ref. [23] for more details on the numerical simulations.).

Since a rotation among the MZMs preserves the total fermion parity [42,43], the holonomy W can have a nontrivial parity signature Δp only if more than one fermion is associated with the MZMs in the dark subspace. This condition is met if $N \geq 5$.

For small areas A of the enclosed loop in phase space, $\Delta p \propto A^2$ depends on the infinitesimal Wilson loop operator w only. Figure 3(a) displays the PDF of the normalized parity signature $\Delta p/A^2$ for $N = 5, \ldots, 12$, using the random-matrix model (6). The asymptotic distribution at small Δp is proportional to $(\Delta p)^{\min(N-4,8)/2-1}$ for N even and $(\Delta p)^{\min(N-3,8)/2-1}$ for N odd, while it decays algebraically $\propto (\Delta p)^{-7/4}$ at large Δp. For repeated small-area loops with cumulative area $ZA \gg 1$, the distribution converges toward the results shown in Fig. 3(c). For $N = 5, 6$, the distribution diverges as $(\Delta p)^{-1/2}$ for $\Delta p \to 0$ and is finite at $\Delta p = 1$. For larger N, the distribution is finite at $\Delta p = 0$ and zero at $\Delta p = 1$. In the limit of a large loop area A, Δp is symmetrically distributed around $\Delta p = 0.5$, see Fig. 3(e), and becomes more peaked at $\Delta p = 1/2$ upon increasing N.

Charge signature.—An alternative method to observe the non-Abelian evolution involves a measurement of the charge on the QD. Hereto, (i) the system is initialized in a unique reference state, (ii) a shape-space loop is performed, and (iii) the time-averaged charge $\bar{Q}$ of the QD is measured after the coupling coefficients v_j are diabatically changed, e.g., by suddenly changing the transparency of some of the tunnel contacts to the MZMs [44]. Measurement of the time-averaged charge on a QD is possible with established techniques [45–48]. The diabatic change of the v_j is necessary because it drives the system into a nonequilibrium state with a time-averaged dot charge that depends on the state of the dark MZMs before the quench. The signature of the non-Abelian time evolution is the difference $\Delta\bar{Q} = \overline{Q(W)} - \overline{Q(\mathbf{1})}$ of the time-averaged dot charge with and without performing a closed loop in shape space at stage (ii). An expression for $\Delta\bar{Q}$ in terms of W is derived in [23].

The charge signature depends on the resonant energy ϵ and is maximal for $\epsilon/\eta \sim 4$ [23]. Unlike the parity signature Δp, the charge signature $\Delta\bar{Q}$ is linear in A for small A. The charge signature distribution $\Delta\bar{Q}$ depends on N and on the type of diabatic quench used to obtain the nonequilibrium state. Figure 3 (right) shows the PDF $\Delta\bar{Q}/A$ for selected values of N, for the case that diabatic change of the coupling coefficients v_j is obtained by suddenly decoupling two MZMs from the dot. (The charge signature $\Delta\bar{Q} = 0$ if only one MZM is suddenly decoupled [23].) The distribution shows a logarithmic singularity at $\Delta\bar{Q} = 0$ and has a power-law dependence $\propto |\Delta\bar{Q}|^{-5/2}$ for large $|\Delta\bar{Q}|/A \gg 1$. The logarithmic singularity persists for repeated infinitesimal loops with cumulative area $ZA \gg 1$ and for large loops with enclosed area $A \gg 1$, cf. Figs. 3(d) and (f). It dominates the distribution such that the dependence on N is weak. Decoupling three or more but fewer than $N - 2$ MZMs results in a nondivergent density at $\Delta\bar{Q} = 0$ [23].

MZMs vs Andreev bound states (ABSs).—Superconductor contacts may host zero-energy ABS that mimic MZMs [12,13]. Although ABSs need not be pinned to zero energy, for weak coupling to the dot, an ABS that is accidentally at zero energy $\ll \eta$ will remain there if the dot shape is changed. An ABS may be seen as consisting of two MZMs. The replacement of MZMs by ABSs has no effect if the two MZMs making up the ABS have very different coupling strength to the dot. If both MZMs couple to the dot with equal strength, their effect is to change the effective number N of MZMs involved in the holonomy W. A strong signature distinguishing MZMs from ABSs results from the charge signature: pinching off one (two) contacts with MZMs has no charge signature (a logarithmic divergence around zero), while pinching off one (two) contacts with ABSs results in a logarithmic divergence (a finite density) around zero. The parity signature strongly distinguishes five and six MZMs from more than six MZMs from its behavior around $\Delta p = 0, 1$. The distinctions are based on the associated ground-state degeneracy, similar to the topological Kondo effect [49].

Concluding remarks.—We have shown that weakly coupling multiple Majorana zero modes to a chaotic QD

leaves a dark subspace of zero-energy modes if the Fermi energy is close to a resonance of the QD. Tuning the shape of the chaotic QD leads to a nontrivial evolution inside the dark subspace, which has observable signatures with universal PDFs. Since the single-particle QD states are nondegenerate, our conclusions remain valid if Coulomb repulsion on the QD considered. The same applies, qualitatively, for Andreev reflections at the QD boundaries, although the precise PDFs may differ in this case, because Andreev reflections change the symmetry class of the QD Hamiltonian to Cartan class D [10].

Estimating the relevant energy scales [23], we expect that our proposal is challenging but within reach of the InAs/Al platform [50]. Another near-term experimental study could utilize "poor man's" Majorana fermions [51–53] or other types of degenerate qubits [54–59] interfaced by a single, chaotic element.

We acknowledge support by the European Research Council (ERC) under the European Union's Horizon 2020 research and innovation program under Grant Agreement No. 856526, and from the Deutsche Forschungsgemeinschaft (DFG) project Grant No. 277101999 within the Collaborative Research Center (CRC) network TR 183 (subprojects A02, A03, C01, and C03), the Danish National Research Foundation, the Danish Council for Independent Research | Natural Sciences, and a research grant (Project 43951) from VILLUM FONDEN.

[1] Y. G. Sinai, Russ. Math. Surv. **25**, 137 (1970).
[2] O. Bohigas, M. J. Giannoni, and C. Schmit, Phys. Rev. Lett. **52**, 1 (1984).
[3] E. P. Wigner, Ann. Math. **62**, 548 (1955).
[4] F. J. Dyson, J. Math. Phys. (N.Y.) **3**, 140 (1962).
[5] A. F. Andreev, J. Exp. Theor. Phys. **19**, 1228 (1964), http://www.jetp.ras.ru/cgi-bin/e/index/e/19/5/p1228?a=list.
[6] A. Altland and M. R. Zirnbauer, Phys. Rev. Lett. **76**, 3420 (1996).
[7] J. A. Melsen, P. W. Brouwer, K. M. Frahm, and C. W. J. Beenakker, Europhys. Lett. **35**, 7 (1996).
[8] W. Belzig, C. Bruder, and G. Schön, Phys. Rev. B **54**, 9443 (1996).
[9] C. W. J. Beenakker, in *Quantum Dots: a Doorway to Nanoscale Physics* (Springer, Berlin, Germany, 2005), pp. 131–174.
[10] A. Altland and M. R. Zirnbauer, Phys. Rev. B **55**, 1142 (1997).
[11] D. Aasen, M. Hell, R. V. Mishmash, A. Higginbotham, J. Danon, M. Leijnse, T. S. Jespersen, J. A. Folk, C. M. Marcus, K. Flensberg, and J. Alicea, Phys. Rev. X **6**, 031016 (2016).
[12] H. Pan and S. Das Sarma, Phys. Rev. Res. **2**, 013377 (2020).
[13] E. Prada, P. San-Jose, M. W. A. de Moor, A. Geresdi, E. J. H. Lee, J. Klinovaja, D. Loss, J. Nygård, R. Aguado, and L. P. Kouwenhoven, Nat. Rev. Phys. **2**, 575 (2020).
[14] D. Rainis, L. Trifunovic, J. Klinovaja, and D. Loss, Phys. Rev. B **87**, 024515 (2013).
[15] M. T. Deng, S. Vaitiekėnas, E. B. Hansen, J. Danon, M. Leijnse, K. Flensberg, J. Nygård, P. Krogstrup, and C. M. Marcus, Science **354**, 1557 (2016).
[16] There is no non-Abelian evolution if $N = 3$ or $N = 4$: if $N = 4$ the basis change (3) amounts to a phase shift of the complex fermion $\Gamma_1 + i\Gamma_2$; if $N = 3$, the dark Majorana mode Γ_1 must be supplemented with an additional Majorana mode not coupled to the dot and the same conclusion applies.
[17] B. L. Altshuler and B. D. Simons, in *Mesoscopic Quantum Physics*, edited by E. Akkermans, G. Montambaux, J.-L. Pichard, and J. Zinn-Justin (North-Holland, Amsterdam, 1995).
[18] T. Guhr, A. Müller-Groeling, and H. A. Weidenmüller, Phys. Rep. **299**, 189 (1998).
[19] I. Aleiner, P. Brouwer, and L. Glazman, Phys. Rep. **358**, 309 (2002).
[20] K. B. Efetov, Phys. Rev. Lett. **74**, 2299 (1995).
[21] The dimensionless gate voltages x, y can be identified experimentally by comparing conductance autocorrelation measurements as a function of gate voltage to predictions from random-matrix theory.
[22] F. Wilczek and A. Zee, Phys. Rev. Lett. **52**, 2111 (1984).
[23] See Supplemental Material at http://link.aps.org/supplemental/10.1103/PhysRevLett.132.036604 for details on the derivation of the Wilson loop operator, parity signature, and charge signature. We provide analytical expressions thereof. For both parity and charge signature, we discuss an additional protocol. We further include numerically sampled distribution functions and derive analytically their limiting behavior for small area $A \ll 1$. Finally, we analyze the experimental feasibility, which includes Refs. [24–30].
[24] T. Karzig, W. S. Cole, and D. I. Pikulin, Phys. Rev. Lett. **126**, 057702 (2021).
[25] A. Bargerbos, M. Pita-Vidal, R. Žitko, J. Ávila, L. J. Splitthoff, L. Grünhaupt, J. J. Wesdorp, C. K. Andersen, Y. Liu, L. P. Kouwenhoven, R. Aguado, A. Kou, and B. van Heck, PRX Quantum **3**, 030311 (2022).
[26] K. Snizhko, R. Egger, and Y. Gefen, Phys. Rev. Lett. **123**, 060405 (2019).
[27] G. Ithier, E. Collin, P. Joyez, P. J. Meeson, D. Vion, D. Esteve, F. Chiarello, A. Shnirman, Y. Makhlin, J. Schriefl, and G. Schön, Phys. Rev. B **72**, 134519 (2005).
[28] I. L. Aleiner and V. I. Fal'ko, Phys. Rev. Lett. **87**, 256801 (2001).
[29] B. I. Halperin, A. Stern, Y. Oreg, J. N. H. J. Cremers, J. A. Folk, and C. M. Marcus, Phys. Rev. Lett. **86**, 2106 (2001).
[30] J.-H. Cremers, P. W. Brouwer, and V. I. Fal'ko, Phys. Rev. B **68**, 125329 (2003).
[31] The Gaussian unitary ensemble description also requires either the absence of spin-orbit coupling in the dot or the presence of sufficiently strong spin-orbit coupling. Without spin-orbit coupling the in-plane magnetic field must be large enough that tunneling between dot and superconductor is spin-polarized. If these conditions are not satisfied, the random-matrix ensemble in the dot may deviate; see

Refs. [28–30] for a discussion of the random-matrix theory for a dot with weak spin-orbit coupling.
[32] We expect the algebraic decay to be cut off for $\lambda \gtrsim \delta^2/\eta^2$ because at this point the splitting of the MZMs from coupling to the nearest nonresonant level ε_{m-1} or ε_{m+1} is comparable to the splitting from the coupling to the resonant level ε_m.
[33] M. V. Berry and P. Shukla, J. Phys. A **51**, 475101 (2018).
[34] M. V. Berry and P. Shukla, J. Stat. Phys. **180**, 297 (2020).
[35] M. V. Berry and P. Shukla, J. Phys. A **53**, 275202 (2020).
[36] A.-G. Penner, F. von Oppen, G. Zaránd, and M. R. Zirnbauer, Phys. Rev. Lett. **126**, 200604 (2021).
[37] K. Flensberg, Phys. Rev. Lett. **106**, 090503 (2011).
[38] S. Plugge, A. Rasmussen, R. Egger, and K. Flensberg, New J. Phys. **19**, 012001 (2017).
[39] T. Karzig, C. Knapp, R. M. Lutchyn, P. Bonderson, M. B. Hastings, C. Nayak, J. Alicea, K. Flensberg, S. Plugge, Y. Oreg, C. M. Marcus, and M. H. Freedman, Phys. Rev. B **95**, 235305 (2017).
[40] M. I. K. Munk, J. Schulenborg, R. Egger, and K. Flensberg, Phys. Rev. Res. **2**, 033254 (2020).
[41] J. F. Steiner and F. von Oppen, Phys. Rev. Res. **2**, 033255 (2020).
[42] J. D. Sau, D. J. Clarke, and S. Tewari, Phys. Rev. B **84**, 094505 (2011).
[43] T. Karzig, Y. Oreg, G. Refael, and M. H. Freedman, Phys. Rev. X **6**, 031019 (2016).
[44] This charge signature is based on the nonequilibrium occupation of the quantum dot, which is distinct from other approaches to measure the Majorana occupation based on an equilibrium energy shift of a quantum dot level due to coherent tunneling events through a series of MZMs [39–41].
[45] R. J. Schoelkopf, P. Wahlgren, A. A. Kozhevnikov, P. Delsing, and D. E. Prober, Science **280**, 1238 (1998).
[46] A. Aassime, G. Johansson, G. Wendin, R. J. Schoelkopf, and P. Delsing, Phys. Rev. Lett. **86**, 3376 (2001).
[47] J. M. Elzerman, R. Hanson, J. S. Greidanus, L. H. Willems van Beveren, S. De Franceschi, L. M. K. Vandersypen, S. Tarucha, and L. P. Kouwenhoven, Phys. Rev. B **67**, 161308(R) (2003).
[48] Y.-Y. Liu, S. G. J. Philips, L. A. Orona, N. Samkharadze, T. McJunkin, E. R. MacQuarrie, M. A. Eriksson, L. M. K. Vandersypen, and A. Yacoby, Phys. Rev. Appl. **16**, 014057 (2021).
[49] B. Béri and N. R. Cooper, Phys. Rev. Lett. **109**, 156803 (2012).
[50] M. Aghaee *et al.* (Microsoft Quantum), Phys. Rev. B **107**, 245423 (2023).
[51] M. Leijnse and K. Flensberg, Phys. Rev. B **86**, 134528 (2012).
[52] I. C. Fulga, A. Haim, A. R. Akhmerov, and Y. Oreg, New J. Phys. **15**, 045020 (2013).
[53] T. Dvir, G. Wang, N. van Loo, C.-X. Liu, G. P. Mazur, A. Bordin, S. L. D. Ten Haaf, J.-Y. Wang, D. van Driel, F. Zatelli, X. Li, F. K. Malinowski, S. Gazibegovic, G. Badawy, E. P. A. M. Bakkers, M. Wimmer, and L. P. Kouwenhoven, Nature (London) **614**, 445 (2023).
[54] N. Earnest, S. Chakram, Y. Lu, N. Irons, R. K. Naik, N. Leung, L. Ocola, D. A. Czaplewski, B. Baker, J. Lawrence, J. Koch, and D. I. Schuster, Phys. Rev. Lett. **120**, 150504 (2018).
[55] T. W. Larsen, M. E. Gershenson, L. Casparis, A. Kringhøj, N. J. Pearson, R. P. G. McNeil, F. Kuemmeth, P. Krogstrup, K. D. Petersson, and C. M. Marcus, Phys. Rev. Lett. **125**, 056801 (2020).
[56] K. Kalashnikov, W. T. Hsieh, W. Zhang, W.-S. Lu, P. Kamenov, A. Di Paolo, A. Blais, M. E. Gershenson, and M. Bell, PRX Quantum **1**, 010307 (2020).
[57] A. Gyenis, A. Di Paolo, J. Koch, A. Blais, A. A. Houck, and D. I. Schuster, PRX Quantum **2**, 030101 (2021).
[58] A. Grimm, N. E. Frattini, S. Puri, S. O. Mundhada, S. Touzard, M. Mirrahimi, S. M. Girvin, S. Shankar, and M. H. Devoret, Nature (London) **584**, 205 (2020).
[59] P. Campagne-Ibarcq, A. Eickbusch, S. Touzard, E. Zalys-Geller, N. E. Frattini, V. V. Sivak, P. Reinhold, S. Puri, S. Shankar, R. J. Schoelkopf, L. Frunzio, M. Mirrahimi, and M. H. Devoret, Nature (London) **584**, 368 (2020).